

## Transition Energies and Nuclear Levels in $\text{Sm}^{152}$ , $\text{Sm}^{154}$ , $\text{Gd}^{152}$ , and $\text{Gd}^{154}$ as Derived from the Separated Isotopes of Europium\*

J. M. CORK, M. K. BRICE, R. G. HELMER, AND D. E. SARASON  
*Harrison M. Randall Laboratory of Physics, University of Michigan, Ann Arbor, Michigan*  
 (Received April 8, 1957)

Specimens of highly enriched  $\text{Eu}^{151}$  and  $\text{Eu}^{153}$  were irradiated in the Argonne CP-5 reactor and the product isotopes studied in both magnetic and scintillation spectrometers.  $\text{Eu}^{152}$  decays by electron emission to  $\text{Gd}^{152}$  and by  $K$  capture to  $\text{Sm}^{152}$ .  $\text{Eu}^{154}$  emits beta particles leading to  $\text{Gd}^{154}$  but no evidence appeared for positron emission or  $K$  capture leading to  $\text{Sm}^{154}$ . The many conversion-electron lines together with coincidence data allowed the evaluation of the gamma transitions and their arrangement in plausible nuclear level schemes. The beta spectra were resolved by the use of the double-focusing spectrometer. Each of the daughter nuclei is even-even in structure. A comparison is made of the observed lower energy transitions and the prediction from the "collective" model for rotational states.

**N**ORMAL europium consists of two stable isotopes whose masses are 151 (47.8%) and 153 (52.2%). On neutron capture two long-lived radioactive isotopes of europium are produced. Many studies<sup>1</sup> have been made of these activities. Mass spectrometer analyses<sup>2</sup> of the active europium emitter showed it to be composed of two activities of nearly the same half-life. Spectrometer observations of the combined activity could not, except for a fortunate guess, lead to the correct assignment of the many gamma energies.

With the availability of the separated isotopes of europium the possibility of a proper interpretation of all observed conversion electron lines and gamma energies exists. A report<sup>3</sup> on the gamma energies derived from  $\text{Eu}^{152}$  as observed in a scintillation spectrometer has been presented.  $\text{Eu}^{152}$  can decay either by  $K$  capture to  $\text{Sm}^{152}$  or by beta emission to  $\text{Gd}^{152}$ . By using a scintillation crystal alone, the energies cannot be precisely evaluated nor is it possible with certainty to conclude in which of the final nuclei the transition occurs, except as this can be deduced from coincidence measurements.

In the present investigation enriched  $\text{Eu}^{151}$  (92%) and  $\text{Eu}^{153}$  (95%) were irradiated in the maximum flux of the Argonne reactor for one month. The resulting strong sources were studied in both magnetic photographic and scintillation spectrometers.

Some thirty well-defined electron lines whose energies are presented in Table I are observed for  $\text{Eu}^{152}$ . In addition, the energies of eight Auger electron lines have been evaluated, yielding values between 31.7 and 39.9 kev. It is apparent that certain groups of electron lines

have energy differences characteristic of the electronic binding energies of samarium while other lines are better satisfied by the corresponding differences in gadolinium. The  $K$ - $L$  difference for gadolinium is about 3 kev greater than for samarium, and since the energy of each electron line is good to about 0.2% a fairly certain conclusion can be made of the element in which each gamma transition occurs. When only a single electron line occurs, as is sometimes the case, the proper placement may be aided by coincidence observations with the scintillation spectrometer.

Similarly, the approximately twenty electron lines obtained with  $\text{Eu}^{154}$  are shown in Table II. Since the mass separation was not complete, there was some trace of each of the strong electron lines due to  $\text{Eu}^{152}$  when  $\text{Eu}^{154}$  was studied. These contamination lines are not recorded in the tables. The remarkable similarity between the spectra from the  $\text{Eu}^{152}$  and  $\text{Eu}^{154}$  sources for the energy band from 100 to 700 kev is shown in the reproduction of a composite spectrogram in Fig. 1.

Many of the electron lines for the two sources seem to have not only nearly the same energy but also

TABLE I. Conversion electron energies in kev and their interpretation for  $\text{Eu}^{152}$  (long-lived).

Electron energy	Interpretation	Energy sum	Electron energy	Interpretation	Energy sum
75.4	$K$ Sm	122.3	567	$K$ Sm	614
114.8	$L_2$ Sm	122.1		or $K$ Gd	617
115.3	$L_3$ Sm	122.1	578.0	$L$ Sm	585.7
120.5	$M$ Sm	122.1	612.3	$K$ Sm	659
122.0	$N$ Sm	122.1		or $K$ Gd	662
198.5	$K$ Sm	245.3	645.0	$K$ Sm	691.9
237.7	$L$ Sm	245.4	684.2	$L$ Sm	691.9
243.8	$M$ Sm	245.4	731.8	$K$ Gd	782.0
294.7	$K$ Gd	345.1	773.8	$L$ Gd	782.1
337.0	$L$ Gd	345.1	825	$K$ Sm	872
343.5	$M$ Gd	345.2		or $K$ Gd	875
362.2	$K$ Gd	412.2	922	$K$ Sm	969
398.3	$K$ Sm	445.2	961	$L$ Sm	969
	or $K$ Gd	448.5	1045	$K$ Sm	1092
404.3	$L$ Gd	412.2	1071	$K$ Sm	1118
456.9	$K$ Gd	507.1	1111	$L$ Sm	1119
498.1	$L$ Gd	506.5	1369	$K$ Sm	1416
539.0	$K$ Sm	585.9	1408	$L$ Sm	1416

\* This investigation received the joint support of the Office of Naval Research and the U. S. Atomic Energy Commission.

<sup>1</sup> S. Ruben and M. Kamen, *Phys. Rev.* **57**, 489 (1940); Cork, Shreffler, and Fowler, *Phys. Rev.* **72**, 1209 (1947); see also Hollander, Perlman, and Seaborg, *Revs. Modern Phys.* **25**, 469 (1953); O. Nathan and M. Waggoner, *Nuclear Phys.* **2**, 548 (1957); F. S. Stephens, Jr., thesis, University of California, 1955 (unpublished).

<sup>2</sup> Karraker, Hayden, and Inghram, *Phys. Rev.* **87**, 901 (1952).

<sup>3</sup> L. Grodzins, *Bull. Am. Phys. Soc. Ser. II*, **1**, 163 (1956); H. Kendall and L. Grodzins, *Bull. Am. Phys. Soc. Ser. II*, **1**, 164 (1956).

TABLE II. Conversion electron energies in kev and their interpretation for  $\text{Eu}^{154}$ .

Electron energy	Interpretation	Energy sum	Electron energy	Interpretation	Energy sum
73.0	<i>K</i> Gd	123.2	675	<i>K</i> Gd	725
115.0	<i>L</i> Gd	123.1	686	<i>L</i> Gd	694
115.6	<i>L<sub>3</sub></i> Gd	123.1	709	<i>K</i> Gd	759
121.2	<i>M</i> Gd	123.1	825	<i>K</i> Gd	875
122.5	<i>N</i> Gd	123.0	or 872	<i>K</i> Sm	872
198.1	<i>K</i> Gd	248.3	949	<i>K</i> Gd	999
239.8	<i>L</i> Gd	248.2	or 996	<i>K</i> Sm	996
246.5	<i>M</i> Gd	248.5	958	<i>K</i> Gd	1008
484.9	<i>K</i> Gd	535	1000	<i>L</i> Gd	1008
or 542.0	<i>K</i> Sm	532	1231	<i>K</i> Gd	1281
or 643.7	<i>K</i> Gd	592	1273	<i>L</i> Gd	1281
	<i>K</i> Sm	589			
	<i>K</i> Gd	694			

similar intensities. This shows the futility of attempting a solution by using unseparated isotopes. An estimate of the contamination of  $\text{Eu}^{152}$  in the  $\text{Eu}^{154}$  is shown by observing the relative intensity of the line at 75.4 kev which is a *K* line for a  $\text{Sm}^{152}$  gamma ray at 122.2 kev. Similarly the conversion lines for the 345.1-kev gamma in  $\text{Gd}^{152}$  appears on the  $\text{Eu}^{154}$  photographic plates. No trace of the  $\text{Eu}^{154}$  lines was noticeable on the  $\text{Eu}^{152}$  plates. This is due to the relatively small capture cross section for neutrons in  $\text{Eu}^{153}$  compared with their capture in  $\text{Eu}^{151}$ .

The gamma rays in Gd and Sm as derived from the electron energies are listed in Table III. Certain of these are expressed with confidence where both *K* and *L* lines are observed. When only single lines are observed, the assignment to the correct daughter isotope and hence the correct energy is dependent upon coincidence observations. In a very few cases this information is not certain and alternate values are given for the gamma-ray energy.

The scintillation spectrometer was used to obtain three types of data. With the specimen of  $\text{Eu}^{152}$  near the crystal a "singles" curve showing peaks as presented in Curve A, Fig. 2, is obtained. Now by inserting the source in a cylindrical hole in the top of the crystal, a "sum" curve is obtained. This shows the additive

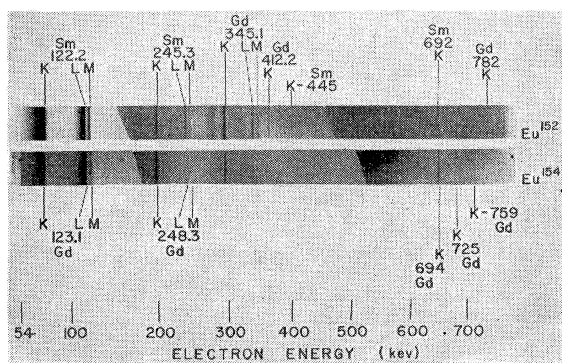
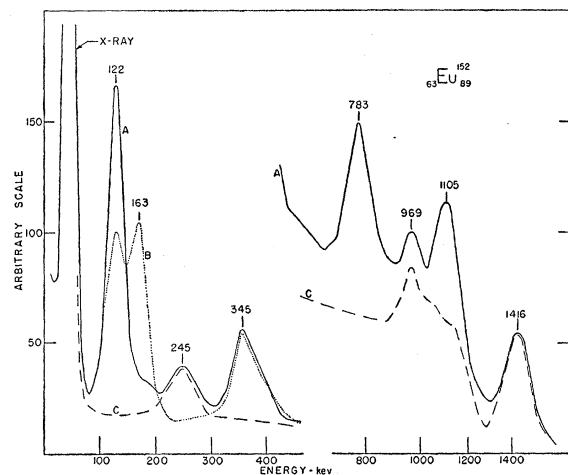
FIG. 1. Electron spectra for sources of  $\text{Eu}^{152}$  and  $\text{Eu}^{154}$  for energies from 100 to 700 kev.

TABLE III. Summary of gamma-ray energies in kev as derived from electron conversion lines.

$\text{Eu}^{152}$		$\text{Eu}^{154}$	
$^{62}\text{Sm}_{90}^{152}$	$^{64}\text{Gd}_{88}^{152}$	$^{62}\text{Sm}_{92}^{154}$	$^{64}\text{Gd}_{90}^{154}$
122.2	345.1		123.1
245.3	412.2		248.3
585.8	507.0		694.0
691.9	782.0		1008
969			1281
1118			
1416			
Other energies (Single conversion line, coincidence data)			
445.2			535
614	or 617		592
659	or 662		725
872	1100		759
1092			875
1170			999

effect of combining certain energies that are in immediate sequence such as the x-ray at 41 kev and the gamma ray at 122 kev to give a new peak at 163 kev, as shown in Curve B. Coincidence data are observed between beta energies and the complete gamma spectrum and between individual gamma peaks and the remaining gamma energies.

Those gamma transitions that are in coincidence with betas must occur in gadolinium, since no positron emission could be found from either source and *K* capture yields only x-ray conversion electrons. By interposing various thicknesses of aluminum between the source and detector, the approximate energy of the coincident betas was established. For example, in the  $\text{Eu}^{152}$  source the 345-kev gamma ray shows strong coincidence with beta rays of energy greater than 400 kev. The 781-kev peak is in strong coincidence with beta energies less than 400 kev and in weak coincidence with higher energy betas. Those gamma transitions

FIG. 2. Scintillation spectrometer data for  $\text{Eu}^{152}$ . (a) Singles distribution; (b) summation peaks; (c) coincidence peaks with the 122-kev gamma ray.

not in coincidence with betas are assumed to be in samarium.

Gamma-gamma coincidences are observed for each source. Curve *C* in Fig. 2 shows the coincidences between the 122-keV gamma ray and gamma rays of other energies. A resolution of the curves shows coincidences at 245, 872, 969, 1118, and 1416 keV. This leads to the placement of the 872-keV gamma ray in samarium even though only a single conversion line was measured for it. The 245-keV gamma ray was in coincidence with peaks at 122, 872, and 1170 keV. No coincidence could be observed between it and the 969-, 1118-, and 1416-keV gammas. The 1170-keV gamma ray was not observed by electron conversion but the coincidence peak is strong evidence that it exists. The 445- and 969-keV gamma rays were definitely in coincidence.

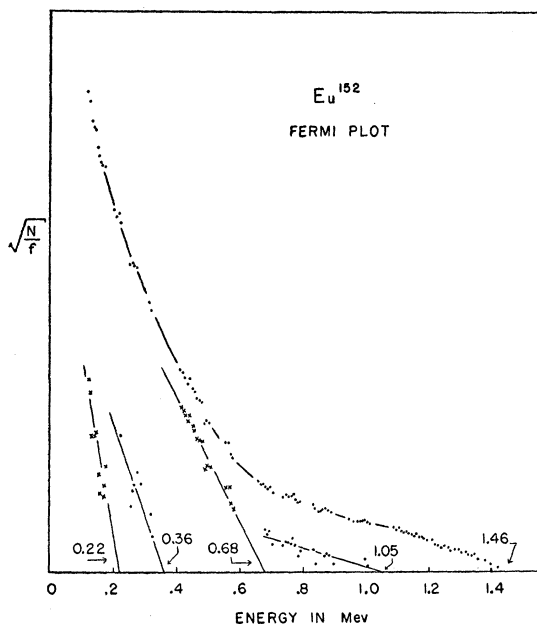


FIG. 3. Fermi plot and analysis of the beta spectrum of  $\text{Eu}^{152}$ .

In  $\text{Gd}^{152}$  the 345-keV gamma ray was found to be in coincidence with peaks at 412, 782, and 1100 keV. The 412- and 782-keV gamma rays were not in coincidence.

The entire  $\text{Eu}^{154}$  gamma spectrum was in coincidence with betas, thus indicating that all of the transitions occurred in  $\text{Gd}^{154}$  and none in  $\text{Sm}^{154}$ . The gamma ray at 123 keV was in coincidence with others at 248, 592, 694, 875, 1281, and possibly 700 and 1000 keV. The 248-keV peak was in coincidence only with energies of 123 and 759 keV. A peak in the region of 700 keV was in coincidence with another at 875 and possibly 1000 keV.

The beta spectra of  $\text{Eu}^{152}$  and  $\text{Eu}^{154}$  were observed with the double-focusing spectrometer. In each case the spectrum was found to be complex, as shown by the Fermi plots in Figs. 3 and 4. The component of highest

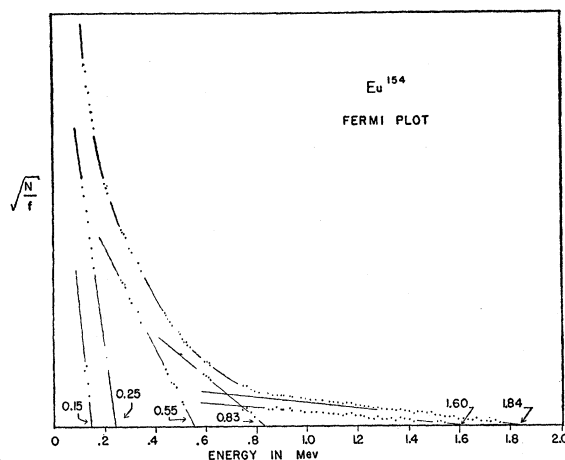


FIG. 4. Fermi plot and analysis of the beta spectrum of  $\text{Eu}^{154}$ .

energy in  $\text{Eu}^{152}$  ( $E_{\text{max}} = 1459$  keV) has the unique first-forbidden shape, while the 680-keV component has the allowed shape. Allowed forms are assumed for the three weaker branches. In  $\text{Eu}^{154}$  no forbidden shapes are evident. In both isotopes the successive subtraction involved in analyses of the Fermi plots lead to relatively large uncertainties in the endpoint energies of lower components. A summary of the energies, branching ratios, and  $\log ft$  values is presented in Table IV.

The relative intensities of a number of the internal conversion lines in both isotopes were measured, both by means of microphotometer traces of the photographic plates and with the double-focusing spectrometer. In  $\text{Sm}^{152}$  the  $K/L$  ratios for the 122- and 245-keV gamma rays are found to be 1.5 and 3.3, respectively, and that for the 345-keV gamma in  $\text{Gd}^{152}$  is 4.6, indicating that all three transitions are electric quadrupole. In  $\text{Gd}^{154}$  the 123- and 248-keV gammas have  $K/L$  ratios of 1.2 and 4.6, respectively, which are again consistent with  $E2$  transitions. For the higher energy gamma rays the  $L$  lines were, in general, too weak to permit reliable intensity measurements.

The decay of  $\text{Eu}^{152}$  and  $\text{Eu}^{154}$  in every case leads to an even-even nucleus, for which the spin of the ground state is zero. The energies of the first excited states of

TABLE IV. Summary of beta transitions in  $\text{Eu}^{152}$  and  $\text{Eu}^{154}$ .

Isotope	Energy (keV)	Rel. abundance %	$\log ft$
$\text{Eu}^{152}$	$1459 \pm 15$	21	11.6
	$1050 \pm 20$	6	11.7
	$680 \pm 20$	51	10.1
	$360 \pm 40$	13	9.7
	$220 \pm 40$	9	9.1
$\text{Eu}^{154}$	$1842 \pm 20$	7	12.4
	$1600 \pm 20$	3	12.1
	$833 \pm 30$	20	10.9
	$554 \pm 30$	30	9.9
	$246 \pm 30$	28	8.9
	$150 \pm 40$	12	8.7

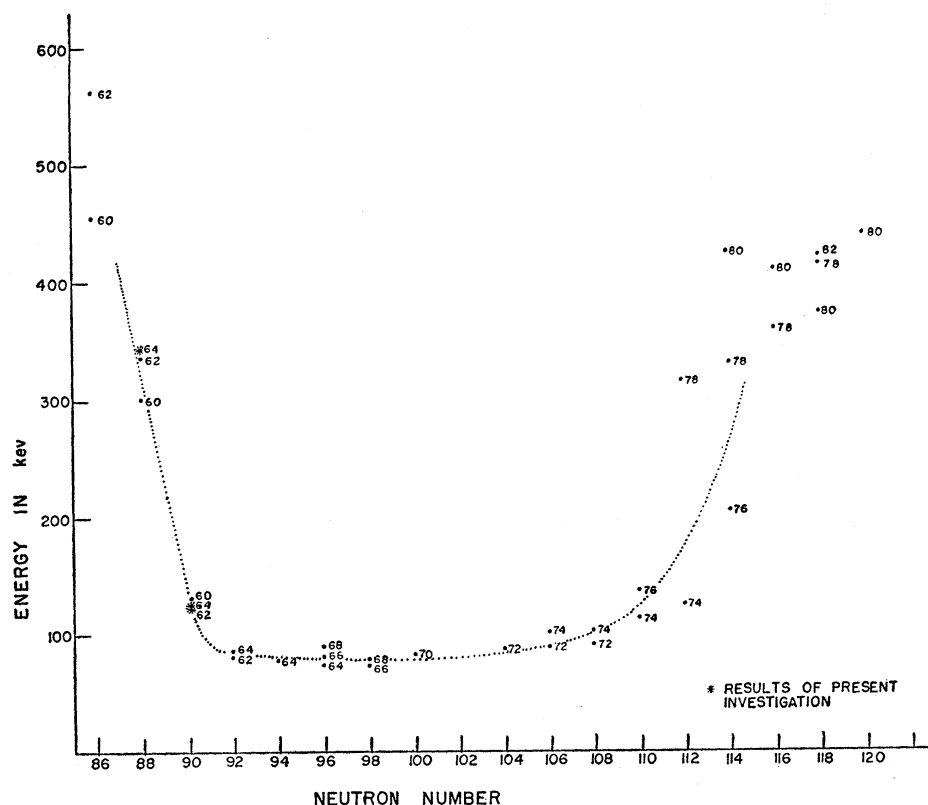


FIG. 5. The energy of first excited states for even-even nuclei as a function of neutron number.

even-even nuclei in this region depend critically upon the neutron number. The data currently available are shown in Fig. 5. The points indicated by asterisks are the results of the present investigation. The strong

spectral similarity shown in Fig. 1 is really due largely to the like structures  $\text{Sm}^{152}$  and  $\text{Gd}^{154}$ , both of which have 90 neutrons.

Level schemes for the daughter isotopes  $\text{Sm}^{152}$ ,  $\text{Gd}^{152}$  and  $\text{Gd}^{154}$  are presented in Figs. 6, 7, and 8. These level schemes are consistent with the available coincidence data, and include all but three of the observed gamma transitions. The first two excited states of  $\text{Sm}^{152}$  and  $\text{Gd}^{154}$  have nearly the same energies, which is not unexpected considering that the two nuclei differ only by a pair of protons. In this region the collective model of the nucleus is expected to apply, predicting a series of rotational excited levels with even spin and parity ( $0^+$ ,  $2^+$ ,  $4^+$ ,  $\dots$ ) and with energies proportional to  $I(I+1)$ . The expected ratio of second to first excited state energies, according to the collective model, is then 10:3, and this ratio is generally observed in the region indicated by the flat part of the curve in Fig. 5, well away from the shell closures at magic numbers.

In  $\text{Sm}^{152}$  and  $\text{Gd}^{154}$ , each with 90 neutrons, the  $E2$  character of the two strong low-energy gamma rays is as expected for transitions between rotational levels, and suggests that the first and second excited states have spins  $2^+$  and  $4^+$ , respectively. The spin assignment of 4 to the second excited state is confirmed, in the case of  $\text{Gd}^{154}$ , by the absence of a beta transition to the ground state, and the 0-2-4 spin sequence has also been established by angular correlation measurements

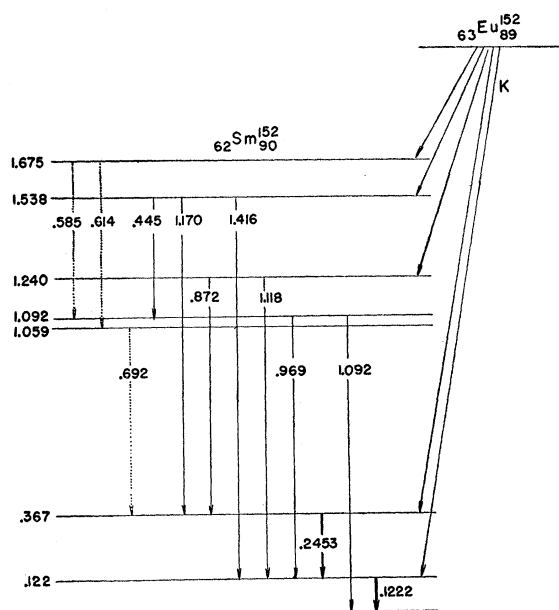


FIG. 6. Level scheme for the  $\text{Sm}^{152}$  nucleus. (Position of dotted transitions not well established.)

in both isotopes.<sup>4</sup> In both cases the ratio of second to first excited state energies is found to be 3:1. The small deviation from the predicted value is attributed to the fact that these isotopes lie just at the lower edge of the band of neutron numbers where the collective model is expected to hold.

In the  $\text{Sm}^{152}$  energy level scheme,  $K$ -capture branches are indicated where the estimated intensities of the gamma transitions seem to warrant them. That  $K$ -capture occurs directly to the 122-keV level is indicated by the fact that the 122-keV gamma forms a strong summation peak with the x-ray alone, as well as with other gamma rays (Curve B, Fig. 2). A comparison of the relative intensities of the 122-keV gamma ray in  $\text{Sm}^{152}$  and the 345-keV gamma ray in  $\text{Gd}^{152}$  indicates that roughly 80% of the  $\text{Eu}^{152}$  decays are by electron capture.

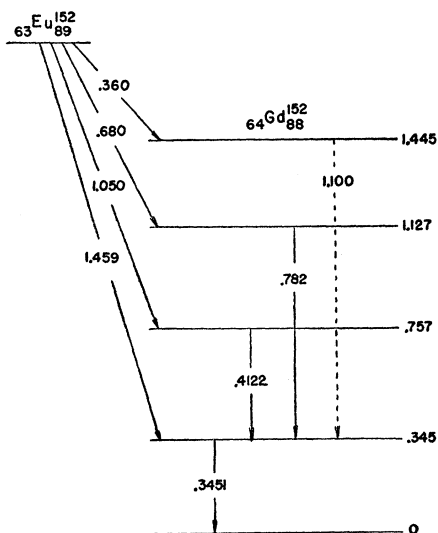


FIG. 7. Level scheme for the  $\text{Gd}^{152}$  nucleus.

In  $\text{Gd}^{152}$  no beta transition to the ground state is observed. The unique first forbidden ( $\Delta I=2$ , yes) shape of the highest energy transition, leading to the 345-keV excited state, suggests that the ground state spin of  $\text{Eu}^{152}$  may be 4, with odd parity. The unusually high  $\log ft$  values of the high-energy beta transitions are probably due to their  $K$  forbiddenness, since they go from a state with  $I=K=4$  to states with  $K=0$  ( $K$  being the projection of the total angular momentum on the nuclear axis of symmetry). The lowest energy beta transition ( $\sim 220$  keV) does not lead to an energy level from which we have observed any deexciting

<sup>4</sup> L. Grodzins (private communication).

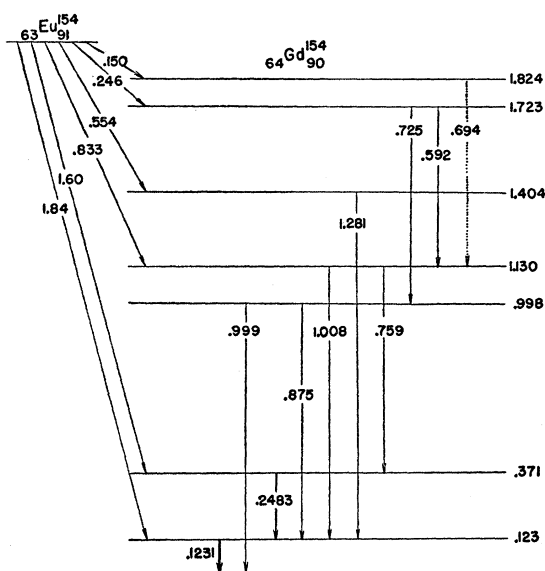


FIG. 8. Level scheme for the  $\text{Gd}^{154}$  nucleus.

gamma radiation and has, therefore, not been shown in the level scheme.

No beta transition to the ground state is observed in  $\text{Gd}^{154}$ . The transitions to the first two excited levels are interpreted as ordinary first-forbidden, suggesting a spin of 3, odd parity, for the  $\text{Eu}^{154}$  ground state. The high  $\log ft$  values for the beta transitions are again attributed to  $K$  forbiddenness.

Coulomb excitation of  $\text{Sm}^{154}$ <sup>5</sup> has led to the observation of a gamma ray at 82 keV. In the present investigation no evidence for this transition appears, nor is there conclusive evidence for other transitions in  $\text{Sm}^{154}$ . Since this isotope is stable, electron capture in  $\text{Eu}^{154}$  should be energetically possible, but it may be concluded that either the branching ratio for this process is small, or most such transitions lead directly to the ground state.

The level schemes proposed here for  $\text{Sm}^{152}$  and  $\text{Gd}^{152}$  are somewhat similar to those proposed<sup>3</sup> by Dr. Grodzins. Certain additional gamma rays are observed while some others are not found as reported. The values of the gamma-ray energies in some cases differ, but at lower values the results from the magnetic spectrometer are undoubtedly more reliable. The level scheme proposed here for  $\text{Gd}^{154}$  is almost the same as that suggested by Stephens, again with some revision of the gamma-ray energies.

<sup>5</sup> N. P. Heydenburg and G. M. Temmer, Phys. Rev. **100**, 150 (1955).

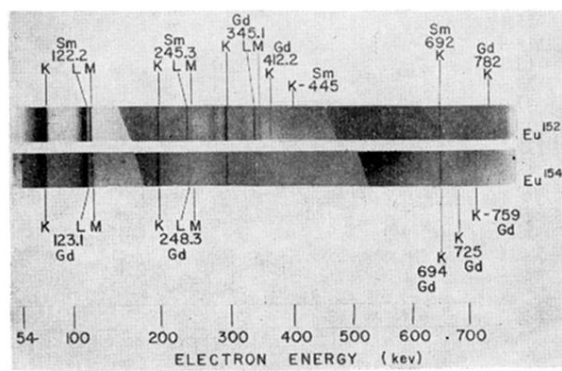


FIG. 1. Electron spectra for sources of  $\text{Eu}^{152}$  and  $\text{Eu}^{154}$  for energies from 100 to 700 kev.